Flood risk assessment of the European road network

Kees C.H. van Ginkel (1,2)*, Francesco Dottori (3), Lorenzo Alfieri (3,4), Luc Feyen (3), Elco E. Koks (2,5)

(1) Deltares, Boussinesqweg 1, 2629 HV Delft, The Netherlands
5   (2) Institute for Environmental Studies, VU University, Amsterdam, The Netherlands
(3) European Commission, Joint Research Centre, Ispra, Italy
(4) CIMA Research Foundation, University Campus of Savona, Savona, Italy
(5) Environmental Change Institute, University of Oxford, Oxford, United Kingdom

*Corresponding author: kees.vanginkel@deltares.nl

ORCIDs:

Kees van Ginkel: 0000-0002-8162-221X

Francesco Dottori: 0000-0002-1388-3303

Lorenzo Alfieri: 0000-0002-3616-386X

15   Luc Feyen: 0000-0003-4225-2962

Elco Koks: 0000-0002-4953-4527

Abstract

River floods pose a significant threat to road transport infrastructure in Europe. This study presents a high-resolution object-based continental-scale assessment of direct flood risk of the European road 20 network for the present climate, using high-resolution exposure data from OpenStreetMap. A new set of road-specific damage functions is developed. The expected annual direct damage from large river floods to road infrastructure in Europe is 230 million euro per year. Compared to grid-based approaches, the object-based approach is more precise and provides more action perspective for road owners, because it calculates damage directly for individual road segments, while accounting 25 for segment-specific attributes. This enables the identification of European hotspots, such as roads in the Alps and along the Sava River. A first comparison to a reference case shows that the new object-based method computes realistic damage estimates, paving the way for targeted risk reduction strategies.

1   Introduction

30 River flooding is among the most damaging natural hazards in Europe. Following disruptive and costly European floods in the year 2000 and between 2009 and 2014, significant advances in continental (and global) scale flood risk modelling have been made (Dankers and Feyen, 2008; Hirabayashi et al., 2013; Kundzewicz et al., 2017; Ward et al., 2013). Although these models provide good estimates of total damage to all land use types, they do not accurately represent damage to

transport infrastructure (Jongman et al., 2012, Bubeck et al., 2019). Flood damage to road infrastructure is still an underexplored, yet important issue (Doll et al., 2014; Merz et al., 2010; Koks et al. 2019). Road flood damages have two dimensions: direct/indirect and tangible/intangible. Direct tangible damage includes clean-up and repair of the physical road assets and traffic management systems, damage to (parked) vehicles, and costs of evacuation and rescue operations; direct intangible damage includes fatalities, injuries, and inconvenience; indirect tangible damages includes damage for companies (and society) suffering from delayed freight and persons, and associated shifts in economic in- and output; indirect intangible damage includes societal disruption and undermined trust in public authorities (Jonkman et al., 2008). Previous studies have shown that transport infrastructure significantly contributes to direct tangible flood losses, usually in the order of 5-10% but in exceptional cases up to 50-60% (Bubeck et al., 2019; Jongman et al., 2012). At the same time, transport disruptions are an important source of indirect economic effects through passenger and cargo delay costs, which may exceed the direct costs (Pregnolato et al., 2017). Furthermore, the accessibility of the road network during flood events is of crucial importance to evacuations and therefore in avoiding casualties (Sohn, 2006). Vehicle-related drowning is the most frequent cause of death during flood disasters (Jonkman and Kelman, 2005). This study focusses on improving the estimates of direct physical asset damage to road infrastructure, but also paves the way for assessment of indirect effects on the continental scale.

Existing continental-scale river flood risk studies do not accurately represent damage to road networks for several reasons. First, these studies are typically grid-based. Damage in a grid cell is determined using a depth-damage curve based on the land use and flood depth in each grid cell. In these grid-based approaches, infrastructure damage is typically determined using the (potential) percentage of infrastructural land use per grid cell in land cover maps such as CORINE or LUISA (Büttner et al., 2014, Rosina et al., 2018). However, transport network infrastructure such as roads and railways are (relative narrow) line elements and take up only a small percentage within a typical grid size for continental-scale modelling (e.g. $100*100$ m^2 in Europe). As these (assumed) percentages are often applied uniformly among the same land-use type, this may result in an overestimation of infrastructure damage when there in reality is no infrastructure, but an underestimation if the infrastructure is there but not enough to be the dominant land-use type. Second, little progress has been made in research on transport-specific damage functions (Hackl et al., 2016) and there is very limited reported data on road damage from flooding. Many studies have pointed out that research on flood vulnerability is underdeveloped (Dottori et al., 2018a), with high associated uncertainty (de Moel and Aerts, 2011) stressing the need for improved vulnerability methods (Winsemius et al., 2013), especially for infrastructure (Jongman et al., 2012). To date, virtually all European-wide flood risk studies (Bouwer et al., 2018, Dottori et al., 2020, Lincke et al., 2019) still rely on the comprehensive set of damage curves proposed by Huizinga (2007), which were developed for (coarse) grid-based assessments, but lack detail for accurate assessment of damage to road networks (Jongman et al., 2012).

Previously, the grid-based approach could be justified by incomplete continental-scale object-based exposure datasets, and insufficient computational power for a more detailed approach. Object-based transport infrastructure datasets such as OpenStreetMap are now nearly complete – by January 2016, most European countries had more than 95% of their roads mapped in OSM (Barrington-Leigh and Millard-Ball, 2017). Also, computational power is no longer a limiting factor, allowing for large-scale high-resolution object-based modelling (Koks et al. 2019), which previously

was limited to smaller scales, such as cities (Chang et al., 2010, Suarez et al., 2005). Object-based damage models, where the damage accounting takes place at the level of objects (in this case: road segments) rather than grid cells, have substantial benefits compared to grid-based approaches. First, the geometric representations have a higher resolution, allowing for more accurate intersects between the exposed roads and the hazard data. Second, object-specific attributes can be used to make more accurate damage estimates (Merz et al., 2010). For example, for an intersect between the road network and an inundation map, it is crucial to differentiate an inundated road from a bridge over the water. The attributes also enable the development of different damage curves for different road types (e.g. motorway or rural road), which may have very different characteristics (e.g. number of lanes, width, quality and maintenance standards). Third, the network properties of roads, enabling graph representations, can be maintained in an object-based approach (Gil and Steinbach, 2008). This enables the study of direct infrastructural flood damage in coherence with other sources of impacts, such as travel delay times from road closures and detours, as well as indirect economic losses from passenger or freight delays.

Koks et al. (2019) proposed a method to study the impacts of climate hazards to road (and rail) infrastructure on the global scale, using data from OSM. The analysis in this global, multi-hazard study used highly stylized damage functions and had to take several assumptions due to information gaps in data-scarce parts of the world. In Europe, object attribute data availability is more complete, allowing for a more detailed approach in this study. Based on an extensive review of road (re)construction costs in Europe, we developed new damage curves by utilizing the available data on road type, number of lanes and the presence of street lighting. Also, we benefit from the higher resolution of flood protection and GDP data in Europe. The increased level of detail allows for presenting the results on the level of individual road segments for hotspot identification. This meets the need of European road owners for GIS-aided vulnerability assessments, for which guidelines have been provided in the ROADAPT project (Bles et al., 2016) but where actual modelling has so far focussed on small spatial scales (e.g. Hackl et al., 2018).

This study introduces an object-based, continental-scale assessment of large-scale river flood risk of the European road network for the present climate. We introduce new damage functions for the object-based approach and compare it to a grid-based approach. To illustrate the richness of the object-based approach, flood hotspots will be identified within the European motorway network. The model results are compared to damage reported for a real flood event near Deggendorf, Germany.

2 Method

Flood risk is commonly defined as a function of flood hazard, exposure and vulnerability (Kron, 2005; Peduzzi et al., 2009). In this study, these components are modelled in three blocks (Fig. 1). Hazard data are taken from the Joint Research Centre's inundation maps of large river floods in Europe (Fig. 1, left). The hazard maps are inputs to two approaches that model exposure and vulnerability: the grid-based approach (Fig. 1, top) and the object-based approach using OSM (Fig. 1, bottom). In total, four combinations of exposure and vulnerability are used to calculate the risk.

Grid-based:

1. CORINE land cover + Huizinga infrastructure damage curve

120   2.   LUISA land cover + Huizinga infrastructure damage curve

Object-based:

        3.   OpenStreetMap + object translation of Huizinga infrastructure damage curve
        4.   OpenStreetMap + new object-based damage curves

These four combinations are selected to enable a comparison between the grid-based and object-based approach, for (1) a land cover grid with poor representation of the road network, (2) a land cover grid with the road network explicitly added to the grid, (3) an object-based approach with the damage curves of the grid-based approach, and (4) an object-based approach with new damage curves. In the remainder of this section, we introduce the flood hazard maps (Sect. 2.1), the grid-based approach (2.2), the object-based approach (2.3), the development of new damage curves (2.4), the sampling procedure (2.5), and the reference case (2.6).
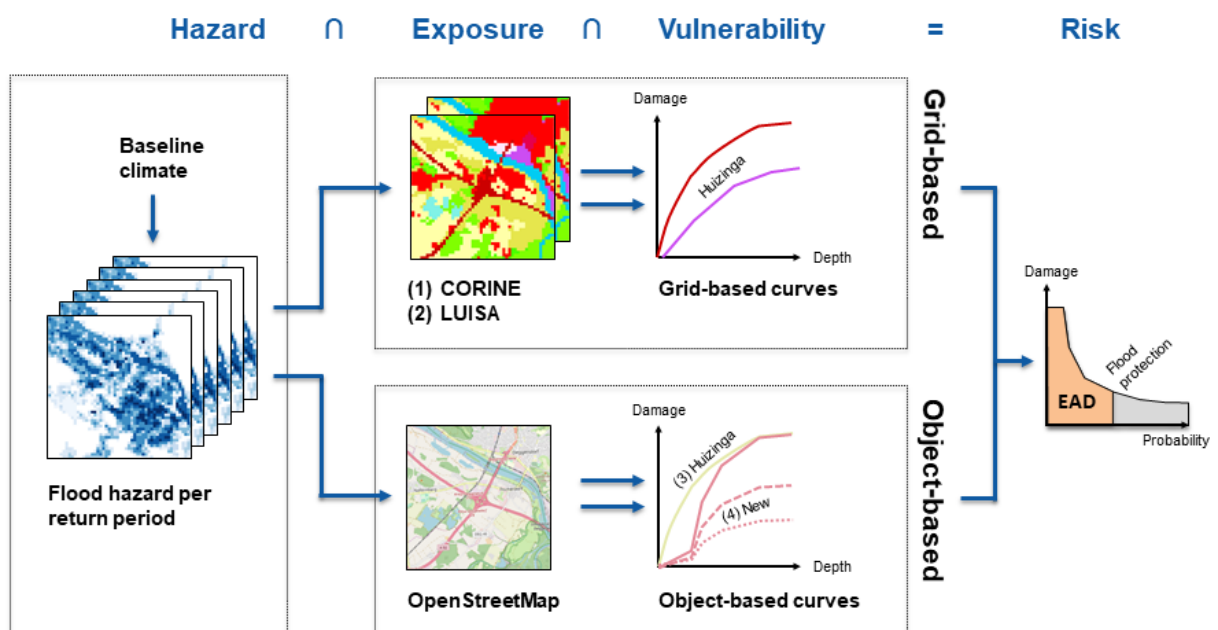
Figure 1 Graphical representation of the risk assessment using the grid-based approach (top-row) with the (1) CORINE and (2) LUISA land cover grids and the object-based approach (bottom-row) with OpenStreetMap and (3) the Huizinga and (4) a set of new damage curves © OpenStreetMap contributors 2019. Distributed under a Creative Commons BY-SA License

2.1 Flood hazard

Flood hazard is represented with a set of inundation maps taken from Alfieri et al. (2015), with a recent update by Dottori et al. (2021) which cover most of the European domain at a grid resolution of 100 m. We provide here a brief description of the inundation maps, noting that no new work was done in the present study to modify these data. The dataset consists of six raster maps of inundation depth corresponding to flood return periods of 10, 20, 50, 100, 200 and 500 years, assuming no flood protection in place (flood protection is considered in the risk assessment step, Fig. S1). These maps represent the inundation depth and extent in all river sections with upstream area larger than 500 km^2. They do not include the effect of pluvial and coastal flooding. They also do not include river and flash flooding in the most upstream catchments, with an upstream area smaller than 500 km^2. Inundation maps were produced by merging the results of thousands of 2D hydraulic simulations along the European river network, based on the hydrodynamic model LISFLOOD-FP (Bates et al.,

2010). The input hydrographs of flood simulations were defined consistently with the peak discharges and flow duration curves of a 25-year long simulation taken from the European Flood Awareness System (Thielen et al., 2009) and based on the hydrological model LISFLOOD (Van der Knijff et al., 2010). Additional details on the methods and models used to produce the maps are described in Alfieri et al. (2014; 2015) and in Dottori et al. (2021), together with some skill assessment of the simulated maps versus official flood maps for different European countries and river basins.

2.2 Grid-based exposure and vulnerability

In the grid-based approach, two different land cover maps are used: CORINE-2012 (version 18.5) and LUISA (version 2). They indicate the dominant land use type in each 100*100 m^2 grid cell. The CORINE land cover map (Büttner et al., 2014) and its predecessors have been used in many European flood risk studies (e.g. Alfieri et al., 2018; Lugeri et al., 2010; Serinaldi and Kilsby, 2017). CORINE, however, overlooks most of the road network (Rosina et al., 2018), because even large motorways typically cover less than 50% of a 100*100 m^2 grid cell, see Fig. S2. Therefore, roads have been manually added to the land cover map in some studies (e.g. Jongman et al., 2012; cf. Meneses et al., 2019). The LUISA land cover map is a spatial and thematic refinement of CORINE-2012 using various additional data sources, such as rasterized object datasets (Rosina et al., 2018). Therefore, motorways and trunk roads that were absent in CORINE are now present in LUISA as coarse grid representations of the original lines. However, due to the 100*100 m^2 resolution of the grid, the actual road width is overestimated in most areas (Fig. S2).

To correct for the underrepresentation of infrastructural land use (and other land use types) in CORINE and LUISA, they assume for each land use class some percentage of infrastructure (Table S1, 2). This assumption follows from Huizinga's suggestion (2007, p. 2-22) to map the damage functions to CORINE using a cross-tabulation by the EEA (2006), which then became the default implementation method. To enable a comparison with the object-based approach, we only consider the percentage of infrastructure per land use class, whereas the contributions of the other damage curves are ignored (Table S1, S2). An implication of these percentages is that, although motorways and trunk roads are mostly missing in CORINE, damage for (local) roads in urban and industrial areas (amongst others) is still calculated, albeit without any explicit spatial reference to the actual road position, but based on their average presence in these land use types. Also, note that in the land cover category 'road and rail networks and associated land', only a 27% infrastructural land use is assumed (Table S1, S2), which to some extents corrects the overestimation of the actual road widths in LUISA. In summary, the grid-based land cover category 'Road and rail networks and associated land' roughly corresponds to the object-based road types 'motorway' and 'trunk road', and the infrastructure percentages in the other grid-based land cover categories roughly correspond to the object-based road types 'primary', 'secondary', 'tertiary' and 'other road'.

2.3 Object-based exposure and vulnerability

This section details the set-up of the object based model (2.3.1) and the application of the Huizinga reference curve (2.3.2) in the object-based approach.

For hydrological reasons, the analysis includes the European Union (EU) 27 member states except Cyprus and Malta; it includes the United Kingdom and the European Free Trade Association countries Liechtenstein, Norway and Switzerland (not Iceland); and includes the (potential)

190 candidate countries Albania, Montenegro, North Macedonia and Serbia (not Turkey). We excluded the EU's remote overseas areas such as the Azores, Canary Islands, Guadeloupe as well as small Islands.

2.3.1 Model set-up

In the object-based approach, all individual OSM road segments are intersected with the flood
195 hazard data, followed by a damage and risk calculation per inundated segment (Fig. 2). To perform this analysis using parallel processing (Fig. 2), the continental OSM 'planet' file is subdivided into 1498 regions, based on the European NUTS-3 division. Per region, every road segment's geometry is simplified to 0.00005° resolution (~5 m in Europe) and intersected with the flood hazard maps per return period, to determine the inundated length and average depth over the inundated part of the
200 segment. Then, the damage to the road segment is calculated for the applicable damage curves. In the post-processing step, the expected annual damage (EAD) is calculated using the trapezoidal rule (Olsen et al., 2015), accounting for flood protection (Fig. S1). In detail, this approach assumes no inundation for return periods of the discharge peaks smaller than that of the flood protection in the same area, while it considers the unprotected inundation maps (Sect. 2.1) for any larger peak (Fig.
205 S1). We used flood protection data developed by Dottori et al. (2020) which integrates the available information on design standards of flood protection (e.g. through technical reports) with modelled protection standards calculated by Jongman et al. (2014) and Scussolini et al. (2016). Modelled data is selected according to observed and simulated historical flood loss data. In this step, the maximum damage per segment is corrected by linearly scaling the national to the former EU-28 average real
210 GDP per capita (Eurostat, 2019), see section S18 for an example.
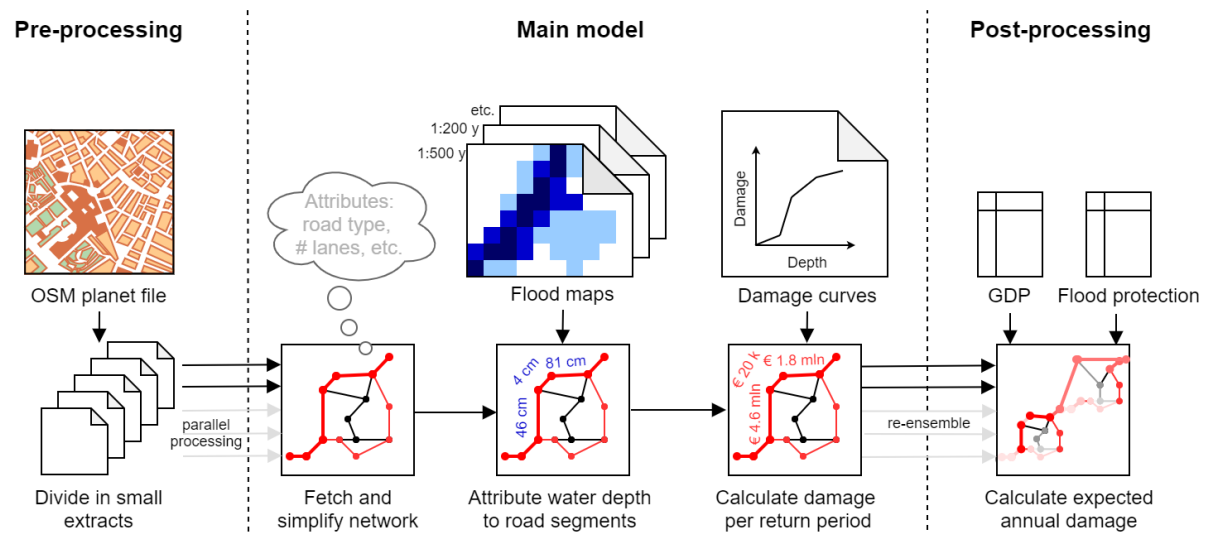
Figure 2 Stylized overview of the object-based approach

Where available, OSM attributes on road type, number of lanes, bridges and lighting is used to
215 improve the damage estimates. Six road types are distinguished following the OSM tagging convention: motorway, trunk, primary, secondary, tertiary and other roads (Table S3). Lane data is available for 90% of the motorways, 60% of trunks, 48% of primary, 23% of secondary, and less than 5% for tertiary and other roads; where unavailable, the countries' median number of lanes per road type is used. For road-water intersections tagged as bridges, no damage to the road is calculated.

220 We acknowledge that bridge failure can be an important source of flood damage (Lamb et al., 2019; Pregnolato, 2019; Vennapusa et al., 2013). Bridge damage, however, does not usually originate from the inundation of the roadway, but rather from scour hole formation to bridge piles and its foundation (Lamb et al., 2019), which cannot be accurately represented in our model.

2.3.2 The Huizinga reference curve

225 A comprehensive set of depth-damage curves has been proposed by Huizinga et al. (Huizinga, 2007; Huizinga et al., 2017), which has been applied in many studies (e.g. Albano et al., 2017; Amadio et al., 2016, 2019; Carisi et al., 2018; Dottori et al., 2018b; Jongman et al., 2012; Prahl et al., 2018). We use the 'EU-average curve' for road infrastructures (Huizinga, 2007). This curve is normally applied in grid-based approaches (see section 2.2), but to enable a comparison to our newly developed curves

230 we also made an object-based translation of the Huizinga curve, by multiplying the per m^2 damage by typical widths of roads in Europe (Table S4).

2.4 New damage curves

The new damage curves cover several aspects of the direct tangible costs. It includes clean-up costs, resurfacing of top and deeper asphalt layers, repairs of road embankments, and where applicable

235 also the repair of electronic signalling and lighting. It does not include structural damage to bridges and tunnels, nor emergency response costs such as the placement of sand bags or signposting of diversions.

To construct the new damage curves, multiple steps are taken. First, we compile an overview of road construction costs, from which we derive a cost bandwidth per OSM road type (Table S5-S7). Expert

240 judgment is used to construct a coherent system of absolute cost values, ratios between the different road types, and scale factor for roads with more or less than the default number of lanes, while accounting for differences in national real GDP per capita. Second, an inventory is created consisting of road clean-up, repair and reconstruction costs expressed as percentages of the road construction costs of the first step (Table S8). Third, repair activities are linked to the road repairs

245 needed following a river flood, derived from literature and photo imagery of river floods in Europe. Fourth, the repair activities and corresponding damage percentages (% of construction costs) are fitted to the depth-damage curves. These depth-damage curves with corresponding narratives are verified in expert workshops with flood risk and transport modelling experts and experts from the Dutch road operator (see acknowledgements). An overview of the damage curves and supporting

250 narratives (reasoning from the road construction and maintenance costs presented below) is given in Fig. S3, S4 and Table S9, S10.

2.4.1 Background data: road construction and repair costs

All costs mentioned in this and the following subsections are linearly scaled using national real GDP per capita (Eurostat, 2019) to represent former EU-28 average 2015 price-levels in euro (€). The

255 model inverses this operation when doing the damage calculation, to tailor the damage to the local context. This is common practice in pan-European flood risk studies (e.g. Alfieri et al., 2016b; Arnell and Gosling, 2016; Ward et al., 2013) and enables comparison with existing studies.

The cost of constructing a new road depends on many factors, such as: road design; accessories like lighting and electronic signalling systems; soil conditions; noise reduction elements; and presence of

260 tunnels and bridges (e.g. Blanc-Brude et al., 2006). For *motorways*, the European Court of Auditors (ECA, 2013) estimates the EU average construction costs at 11.4 million €/km. The cheapest 2x2 lane

motorways with fairly simple road designs are about 3.5 million €/km, the most expensive roads with tunnels, bridges or noise barriers cost about 35 million €/km (ECA, 2013). Other studies report values well within this bandwidth (Carruthers, 2013; Federal Ministry of Transport and Digital Infrastructure, 2016; Heralova et al., 2014; Nijland et al., 2010; Pryzluski et al., 2012), as presented in Table S6. For costs of other road types see Table 1, which is based on literature tabulated in the SI (Table S5-S7). For roads with more (less) than the default number of lanes, we added (subtracted) 25% of costs for each lane, based on Table S5.

We expressed road maintenance and repair costs as a percentage of the construction costs of the corresponding road type (Table S8). Clean-up activities and small repair works are in the order of a few percent of construction costs (Reese, 2003, Archondo-Callao, 2000). Larger scale road improvement and resurfacing is in the order of 10%, whereas major asphalt work and road reconstruction is in the order of 30-40% of construction costs (Carruthers et al., 2013; Archondo-Callao, 2000).

2.4.2 Categories of damage curves

Continental-scale models typically work with functions relating damage to water depth only (Alfieri et al., 2016a; De Moel et al., 2015; Winsemius et al., 2013). Flow velocity, however, is at least as important as water depth for explaining damage to roads (Kreibich et al., 2009; Merz et al., 2010; Thieken et al., 2009). Under low flow velocities (< 0.2 m/s), there is hardly any structural damage to pavements, whereas under high flow velocities (> 2.0 m/s) there is most likely severe structural damage (Kreibich et al., 2009). Indeed, pictures of floods in Europe show that under very quiet flow conditions, a road can remain almost undamaged whereas under flash floods with strong currents, complete reconstruction may be required. The flood hazard maps used in this study represent floods in rivers with an upstream area >500 km^2 whereas large flow velocities are typically found in smaller water courses in steep upstream areas and locally, close to dike-break locations (De Moel et al., 2009). Therefore, we assume that the predicted floods have relatively low flow velocities. We deal with the remaining uncertainty by estimating two depth-damage curves that span the uncertainty of this typical slow flow velocity; one for the low-flow estimate and one for high-flow estimate (i.e. the lower and upper boundary of the relatively slow velocity) that can be reasonably expected for large river floods.

The six new depth-damage curves differentiate between three dimensions: road type, road accessories and flow velocity (Fig. 3). Concerning road type, motorways and trunk roads are distinguished from other roads because of higher driving speeds and maintenance standards, reflected in higher reconstruction costs. Also, these are often built on top of embankments, so that relatively little damage occurs when the top of the road embankment is not yet reached, represented by a concave section in the beginning of curve C1-C4 (Fig. 4). The other road categories (primary, secondary, tertiary and other roads) are usually not built on top of embankments, and their curves (C5,C6) therefore do not have such a concave section. Next, motorways and trunk roads with sophisticated accessories such as electronic traffic management systems, lighting and noise barriers (C1,C2) are differentiated from simple roads without these accessories (C3,C4). This represents the large spread in construction costs between simple and sophisticated motorways and trunk roads (Table S6) and the corresponding extra damage that may occur to the electronic signalling and lighting of sophisticated roads, even under low-flow conditions (Fig. 4). Finally, low-flow conditions (C1,C3,C5) are distinguished from high-flow conditions (C2,C4,C6).
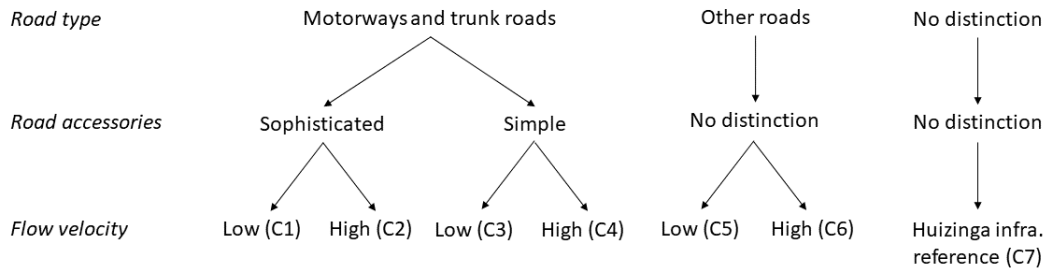
Figure 3 Dimensions used for differentiating the new damage curves (C1-C6) and the reference curve (C7)

2.4.3 New damage curves

The damage curves are expressed as percentage of the road construction costs, see Table 2. They are to be multiplied with the construction cost range per road type (Table 1). This gives the absolute damage as a function of water depth, in former EU-28 averaged, 2015-pricelevel, see Figure 4. A protocol for implementation of the curves can be found in the supplementary information, Sect. S8.

The shapes of the curves are derived from the expected clean-up and repair activities (all percentages refer to % of construction costs) at a given water depth and flow condition. For illustration purposes, we here describe the narratives of curve C3 and C4. Under low flow conditions, simple motorways and trunk roads (C3) exhibit very little damage as long as the top of the 1-m high road embankment is not yet reached. Upon embankment overtopping, a clean-up of the road pavement is required (~1 %). At increasing water depth, the water starts carrying larger debris, requiring a clean-up and minor repair works, till about ~4% at maximum water depth. Under high flow conditions (C4), erosion and instability already causes damage before the road is overtopped. When water starts overtopping the embankment (> 1 m) larger scale road repairs are needed (~10 %) increasing to major repair works and road reconstruction (~35%). For sophisticated roads with electronic signalling, we have assumed that the difference between the low flow (C1) and high flow curve (C2) is smaller, because the electronic signalling (compared to embankments and pavements) is relatively more sensitive to water depth than to flow velocity. All narratives can be found in Table S9.

Table 1 Road construction costs and maximum damage per road type, differentiated between low flow (low flow velocities) and high flow (high flow velocities). The values present the average for the former EU-28, in million 2015-euro per km.

Road type	Lanes [-]	Construction cost range [10^6 €/km]	Max damage (low flow) [-]	Max damage (high flow) [-]	Max damage (low flow) [10^6 €/km]	Max damage (high flow) [10^6 €/km]	Huizinga max dam.[a,d] [10^6 €/km]	Applicable damage curves[d]
			Relative to constr. costs		Absolute values			
Motorway	2*2	3.5 - 35	20% (ac)[b]	22% (ac)[b]	3.9-7.0 (ac)[c]	4.2-7.7 (ac)[c]	0.90	C1, C2
			4% (si)[b]	35% (si)[b]	0.1-0.8 (si)[c]	1.2-6.7 (si)[c]		C3, C4
Trunk	2*2	2.5 - 7.5	20% (ac)[b]	22% (ac)[b]	1.0-1.5 (ac)[c]	1.1-1.7 (ac)[c]	0.60	C1, C2
			4% (si)[b]	35% (si)[b]	0.10-0.20 (si)[c]	0.88-1.75 (si)[c]		C3, C4
Primary	2*1	1.0 - 3.0	5%	35%	0.050-0.150	0.350-1.050	0.25	C5, C6
Secondary	2*1	0.50 - 1.5	5%	35%	0.025-0.075	0.175-0.525	0.225	C5, C6
Tertiary	2*1	0.20 - 0.60	5%	35%	0.010-0.030	0.070-0.210	0.175	C5, C6
Other	1	0.10 - 0.30	5%	35%	0.005-0.015	0.035-0.105	0.075	C5, C6

330 Notes:

a) Huizinga max damage costs [€/km] are obtained by multiplying the m² costs with typical road widths per road type (Table S4).

b) ac = sophisticated road with accessories such as street lighting and electronic signalling; si = simple road, without accessories

335 c) For accessories roads: 50-100% of the construction costs range, for simple roads: 0-50% of the construction costs range

d) The Huizinga max damage is to be combined with the Huizinga damage function, not C1-C6.

Table 2 Damage curves, as percentage of road construction costs.

Curve 1		Curve 2		Curve 3		Curve 4		Curve 5		Curve 6	
Motorways and trunk roads (with embankment)								Other roads (no embankment)			
Sophisticated accessories				Simple roads							
Low flow		High flow		Low flow		High flow		Low flow		High flow	
Depth (cm)	Damage (-)	Depth (cm)	Damage (-)	Depth (cm)	Damage (-)	Depth (cm)	Damage (-)	Depth (cm)	Damage (-)	Depth (cm)	Damage (-)
0	0	0	0	0	0	0	0	0	0	0	0
50	0.01	50	0.02	50	0.002	50	0.015	50	0.015	50	0.12
100	0.03	100	0.06	100	0.004	100	0.04	100	0.025	100	0.2
150	0.075	150	0.1	150	0.025	150	0.2	200	0.035	200	0.28
200	0.1	200	0.12	200	0.03	200	0.25	600	0.05	600	0.35
600	0.2	600	0.22	600	0.04	600	0.35				
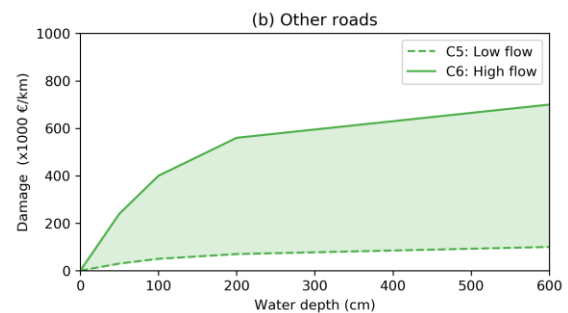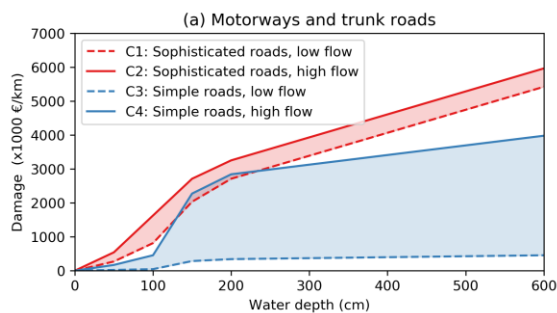
340 **Figure 4 Damage curves for illustrative values of road construction costs, in euros per km.**
(a) The curves for sophisticated roads (C1 and C2) are combined with the 75th percentile of the construction cost range for 2*2 lane motorways, and the curves for simple roads (C3 and C4) with the 25th percentile.
(b) These curves (C5 and C6) are combined with the 50th percentile of the construction costs of primary roads.
The price level is the average of the former EU-28, in 2015.

345 **2.5   Sampling the uncertainty space**

The damage estimates come with considerable uncertainty, which primarily originates from the bandwidth of the construction costs and the space between the upper and lower estimate of the flow velocity. This uncertainty space is sampled to obtain (1) a deterministic estimate of the expected annual damage, as well as (2) a probability distribution around this estimate. Motorways

350 and trunk roads with street lighting tags in OSM are assumed to have sophisticated road accessories; damage curves C1 and C2 are applied (Fig. 3) in combination with a construction cost sample from 50-100% of the range (Table 1, note C). In the probabilistic sample, per road segment, a random choice is made between the 50%, 75% and 100% percentiles of the range, and in the deterministic sample, 75% is used for each segment. For motorway and trunk roads without street lighting tags,

355 simple road designs are assumed; damage curves C3 and C4 are applied in combination with a random choice from the 0%, 25% and 50% percentiles of the range in the probabilistic, and 25% in the deterministic sample. For all other road types, for each road segment a random choice is made from the entire construction cost range in the probabilistic approach, and 50% in the deterministic sample. To account for the uncertainty in flow velocity in the probabilistic approach, we quasi-

360   random sample 1000 z-scores assuming a normal distribution with the low flow curve at -2 standard deviations and the max flow curve at +2 standard deviations from the mean flow damage. This assumption was made because of the lack of reference data. This results in 100 estimates of the damage per segment (one for each z-score). Per z-score, the damage of all road segments is aggregated to construct Figure 5d. In the deterministic sample, the average of the min and max flow

365   curves is taken.

2.6   Comparison to reference case

As a reference, we compare our model to road repair data reported by the Bavarian Government (Table S17). On 4 and 5 June 2013, an approximately 1:100 year flood caused a dike breach near the confluence of the River Danube and its tributary: the River Isar, close to the town of Deggendorf. The

370   inundated area spanned the cloverleaf junction of the motorways A92 and A3, as well as 6.6 km of the A3 and 2.8 km of the A92 (Fig. 8). Both roads have 2*2 lanes + 2 safety lanes and are 30 m and 26 m wide, respectively. They are accurately represented as 2*2 motorways in OSM. The roads are located on embankments and have a fairly simple road design, i.e. no lighting or electronic signalling. We estimate water depths and damage to these roads and surrounding area from reports

375   (Rogowsky, 2016), video's, photos and satellite imagery (Table S17). We then mask the 1:10 year flood hazard map (which better resembled the reported inundation than the 1:100 year flood map) over the extent of the observed inundation and calculate the damage using the object-based model. This offers a partial validation of the damage curves for motorways with simple design, more data is needed to validate the entire methodology.

380 ## 3   Results

This section presents the flood risk of the European road network. Firstly, the object-based approach is compared to the grid-based approach, using the Huizinga damage curves in both approaches (Sect. 3.1). Secondly, the new damage curves are used in the object-based approach, to give more precise estimates of the aggregated road damage in Europe and to give insight into the uncertainty

385   surrounding these estimates (3.2). Thirdly, these results are presented on the road segment level to identify flood hotspots in the European highway network (3.3). Fourthly, the model results are put in perspective of the damage reported for the Deggendorf flood event (3.4).

3.1   Grid-based vs. object-based damage for Huizinga damage curve

The grid-based approach estimates the total expected annual damage (EAD) for the CORINE and

390   LUISA land cover map at 536 and 301 million €/y respectively (Fig. 5a), whereas only 228 million €/y is estimated by the object-based approach (Fig. 5b). Both approaches use the same hazard data and both use the Huizinga vulnerability curve, so that the differences are mainly attributable to the exposure data. A surprising observation concerning the exposure data is the large amount of infrastructural damage (65%) attributed to the CORINE land cover type 'water'. This peculiarity

395   originates from Huizinga's suggestion (Huizinga, 2007, p. 2-22) to map the damage functions to CORINE using a land cover cross-tabulation from the European Environment Agency (EEA, 2006, cf. Table S1). The EEA shows that some cells that contain 'water bodies' in CORINE contain 'infrastructure' in a reference map. Consequently, some percentage of infrastructure is assumed for all CORINE water bodies, for which large damage is calculated, because sometimes large 'inundation

400   depths' are modelled for water bodies. This peculiarity was manually removed in the model implementation of LUISA (Table S2), such as in the recent PESETA-IV study (Dottori et al., 2020).

Another difference is the strong increase in damage to 'Road and rail networks and associated land', from 15 million €/y in CORINE to 144 million €/y in LUISA, resulting from integrating the motorway network into the LUISA land cover grid (Rosina et al., 2018).

405   It should be noted that the object-based approach only reports damage to road infrastructure, whereas the grid-based approach also reports damage to rail infrastructure. However, the area occupied by the railway network is usually limited compared to the road network. Moreover, since the very narrow railway line elements have not been explicitly integrated in the LUISA grid (Rosina et al., 2018), they are mostly overseen, and hence their contribution to the LUISA damage is small.

410   Therefore, we assume that LUISA class 'Road and rail networks and associated land' corresponds to the motorway network and that the other LUISA land use classes correspond to the underlying road network. Accordingly, in the grid-based approach, motorways contribute 48% and the underlying road network 52% to the total road infrastructure damage (Fig. 5a). In the object-based approach, motorways contribute 9%, trunk roads 7%, and the underlying road network 85% (Fig. 5b,

415   percentages rounded). This relatively minor contribution of motorways in the object-based approach results from the way in which the Huizinga curve is implemented: damage per square meter is multiplied by the road width. Motorways, however, are relatively more expensive than is to be expected from merely their width. Therefore, the damage to motorways is underestimated in Figure 5b. The other way around, the other road types are less expensive than is to be expected from their

420   width. Therefore, damage to the underlying road network is overestimated in Figure 5b. This emphasizes the need for damage curves that correct for road characteristics beyond only the road width, as used in the next section.
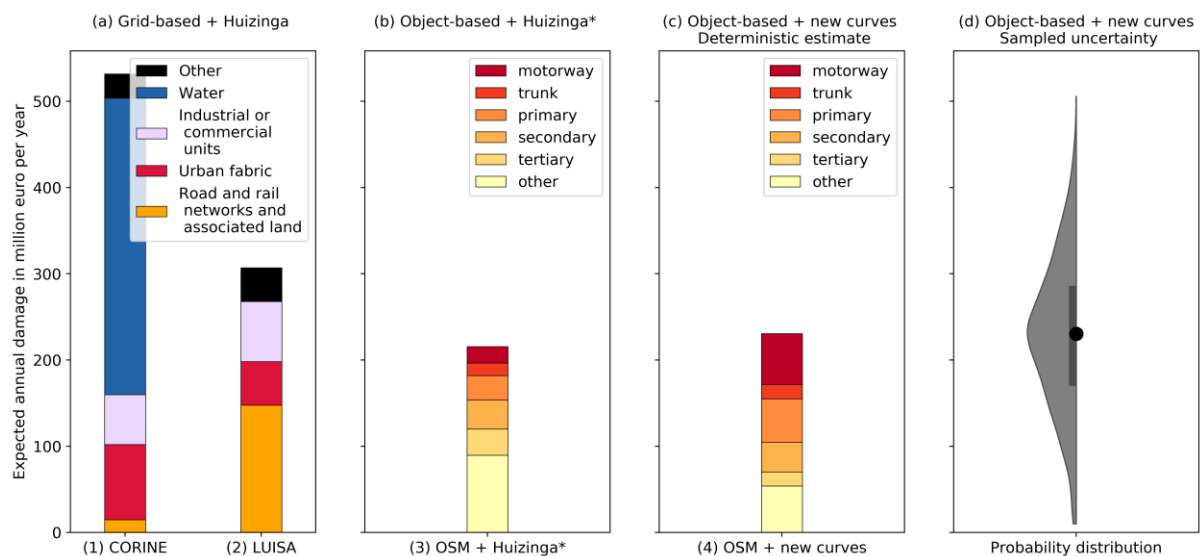
Figure 5 Flood risk of the European road network according to the grid-based and the object-based approach

425   (a) Grid-based approach with (1) CORINE and (2) LUISA + the Huizinga damage curves, per land cover type
(b) Object-based approach + *object translation of Huizinga damage curves (3), per road type
(c) Object-based approach + new damage damage curves (4), deterministic estimate per road type
(d) As (4) with probability density around the deterministic estimate of panel c, black dot indicating the median and thick line indicating the interquartile range

430   ## 3.2   Object-based damage using new damage curves

With the new depth-damage curves the EAD is estimated at 231 million €/y (Fig. 5c), which is again below the grid-based LUISA estimate (301 million €/y, Fig. 5a). The total damage with the new

curves (231 million €/y, Fig. 5c) is somewhat higher than the object-based implementation of the Huizinga damage curve (216 million €/y, Fig. 5b), and the contribution per road type is substantially different. Notably, the contribution of motorways (26%) has become much larger. The other contributions are 7% for trunk, 22% for primary, 15% for secondary, 7% for tertiary and 23% for other roads (Fig. 5c).

The object-based approach also gives insight into the uncertainty surrounding the deterministic estimate of 231 million €/y. The mean of the stochastically generated samples is 229 million €/y and the median is 230 million €/y (Fig. 5d), which approximates the deterministic estimate well. The interquartile range (containing 50% of the samples) is 172 to 284 million €/y. The lower tail (Fig. 5d) is truncated, because outliers in low flow velocity cannot cause damage below zero, whereas at the high tail high flow velocities cause large damage.

Figure 6a shows how the object-based risk (deterministic estimate) is geographically spread over Europe. Germany, France, and Italy are exposed to the highest flood risk (respectively 45, 43, and 23 million €/y, see Fig. S5,S6). In these countries, the risk is concentrated around the rivers that rise in the Alps and then flow through regions with dense road networks, such as the Danube and Rhine flowing through Southern Germany; the Rhone flowing through south-eastern France; and the Po flowing through northern Italy. These three countries have additional flood hotspots in the Elbe, Garonne, and Tiber River basins respectively. Of the top-10 NUTS-2 regions with the largest damage, five are in France and two in Italy (Table S16).

Another concentration of high flood risk is found on the Scandinavian peninsula. This can be partly explained by the high GDP per capita and the relatively large NUTS-regions. However, also when correcting for these factors, we find that the sparse road networks in these countries indeed have the potential to be inundated with large water depths, causing large damage. The regions Pohjois-ja Itä-Suomi (Finland) and Hedmark og Oplland (Norway) are in the top-10 of NUTS-2 regions with the largest risk (Table S16).

Because the value of the exposed assets is scaled to the national GDP per capita, the risk is relatively high in high-income countries. If the risk is expressed as share of the GDP per NUTS-3 region, other high-risk regions emerge: the Central-European countries Czech Republic, Slovakia, and Hungary, but also Croatia and Latvia (Fig. 6b). Although these countries contribute little to the total damage in Europe, the relative impact of road disruptions in these countries is large. Note that these regional (NUTS-3) risk aggregations are influenced by the size of the regions in the NUTS classification; smaller regions show relatively smaller risk in Figure 6. Therefore, aggregation at different levels reveals slightly different spatial patterns (Fig. S7, Table S14,S15,S16).
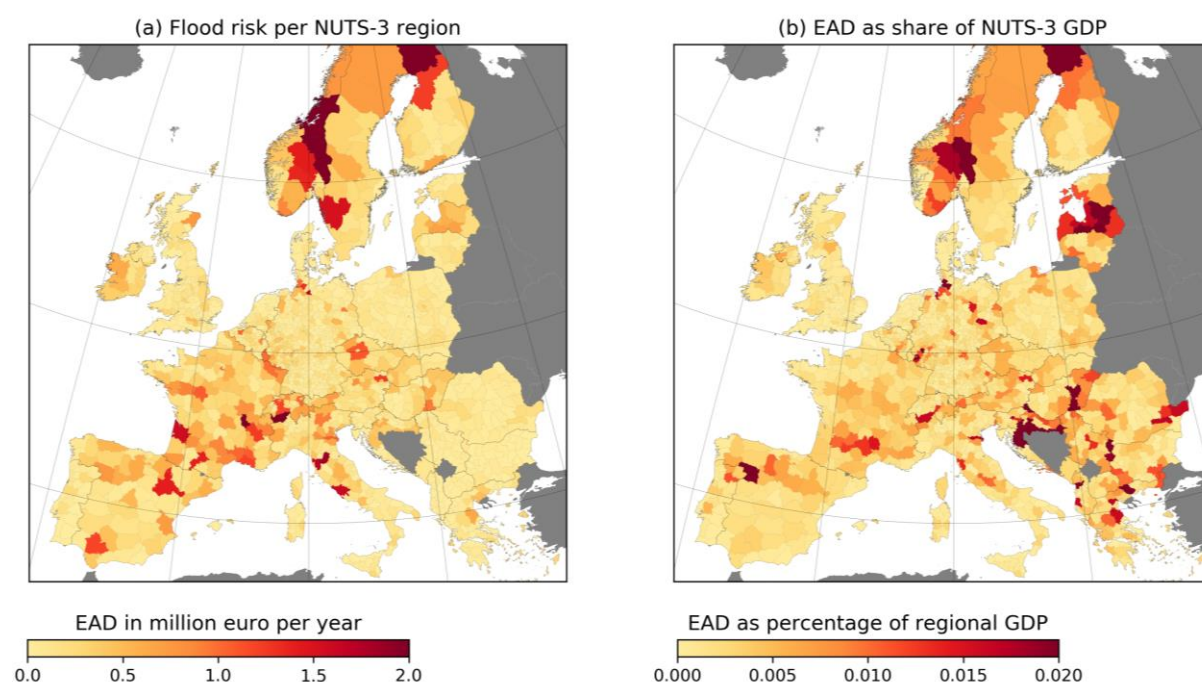
Figure 6 Expected annual damage (EAD) to road infrastructure aggregated by NUTS-3 region. The left-hand panel presents the absolute values, the right-hand panel expresses the EAD as percentage of the GDP per NUTS-3 region.

3.3 Current flood hotspots in the EU transport network

470   The flood risk of all motorways and trunks in the EU road network is now presented on a high-resolution map, see Fig. S8. To illustrate how this map can be used to identify flood hotspots in the EU road network, we highlight three notable regions (Fig. 7).
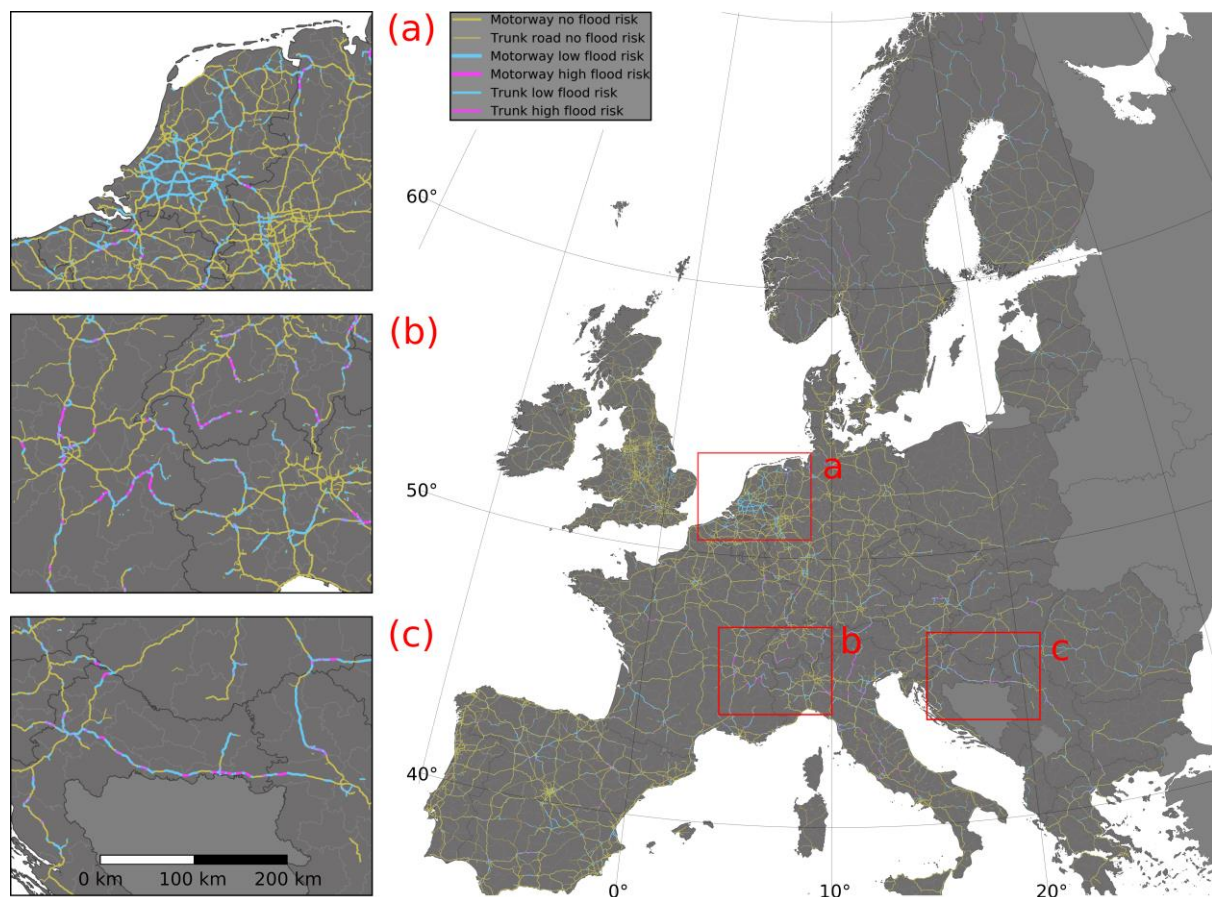
Figure 7 Flood risk of motorways and trunk roads in the European main road network, see Figure S8 for a high-resolution version, which is also made available as shapefile.
(a) The Netherlands
(b) Western Alps in France, Switzerland and Italy
(c) North-western Balkans in Croatia and Serbia
Road geometries © OpenStreetMap contributors 2019. Distributed under a Creative Commons BY-SA License.

The Netherlands stands out in Fig. 7a, because many of its motorways have the potential to be inundated, although at the same time, the aggregated flood risk is among the lower countries in Europe (Fig. S5). This can be explained by the very high river flood protection standards in the country (return period of 1:1000 year or higher in most places), which make the likelihood of flood events very small. However, if dikes did breach, many roads would be inundated with large water depths, causing large damage. Also, this could severely hinder the possibilities for evacuation, especially in the centre of the country.

The Alps are identified as a high-risk region. For example, in France, the model predicts large EAD for the A41 from Grenoble to Chambéry, and the A43 from Chambéry to Sain-Jean-de-Maurienne (Fig. 7b). Both motorways are located in narrow flood plain valleys along rivers. This exposes them to large flood hazards, which is also recognized in local flood risk studies (e.g. Strappazzon and Pierlot, 2017). Similar exposure of motorways can be found in other Alpine regions, such as the A9 from Sion to Montreux (Switzerland), the A22 from Lake Garda to Bolzano (Italy), and the A12 from Landeck via Innsbruck to Kufstein (Austria).

In the Balkans, the E70 motorway from Zagreb (Croatia) to Belgrade (Serbia) is subject to large flood risk (Fig. 7c). This road follows the course of the Sava River for about 400 km. The flood plains of the

Sava River were struck by a large flood in 2014 (International Sava River Basin Commission, 2014). According to our model, the flood waters could hit the motorway at several locations. For some road segments the EAD is notably high. This is primarily the result of a large flood hazard rather than a large value of exposed assets, because the GDP of Croatia and Serbia is below the (former) EU-28 average.

3.4   Deggendorf reference case

As described in Sect. 2.4, the Deggendorf flood event is used as a reference for the damage estimates of the model (Fig. 8). During the flood event, the pavement of the A3 motorway was submerged over 6.6 km because the road embankment was lower than the water level in the surrounding area, resulting in water depth of 0.5 m above the road pavement, on average. After the flood, the A3 was covered with debris (a gas tank, hay bags covered in plastic, wooden logs, plastic bags, pallets), sand, and mud, requiring a major clean-up. At the cloverleaf, there were rifts in the asphalt, requiring small asphalt works. Small strips of asphalt (but not the entire road) were milled and resurfaced. The embankment of the A92 was higher than the embankment of the A3, so that its pavement remained dry over the entire 2.8 km, except a small depression at an underpass with a local road (see Table S17).
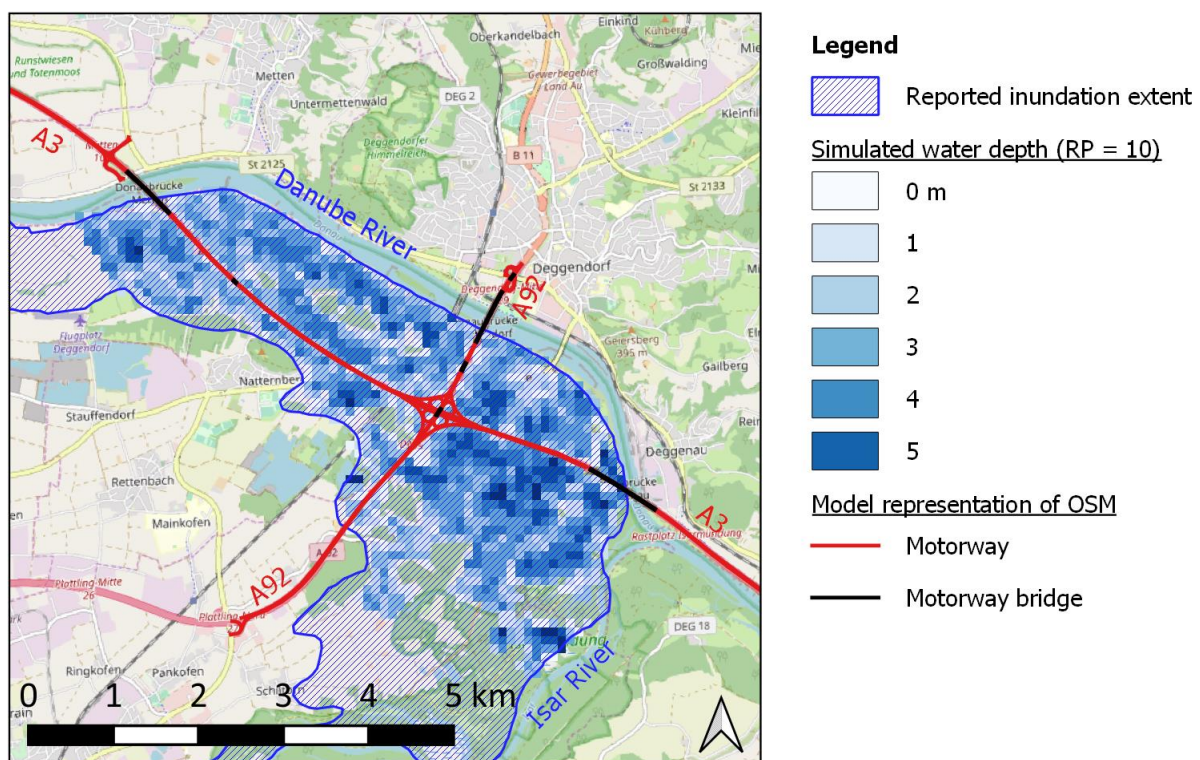
Figure 8 Observed and simulated flood in Deggendorf. Simulated map according to the cropped Return Period (RP) = 10 year flood map (Alfieri et al., 2015), background map © OpenStreetMap contributors 2019. Distributed under a Creative Commons BY-SA License.

The Bavarian State Ministry was granted 3.8 million euro for rehabilitating the Deggendorf cloverleaf junction (Table S17). The model calculates damage of 3.4 million for the low-flow curve (C3) and 28.6 million for the high-flow curve (C4). The video imagery and the limited asphalt damage (Table S17) suggest that flow velocities were relatively low, so that one expects the damage more towards our low-flow than the high-flow damage curve, which is indeed the case.

When interpreting these results, one should consider that German motorways are relatively cheap compared to those in other EU countries (after scaling for GDP, see Table S6); which could imply that rehabilitation works are also relatively cheap (cf. ECA, 2013). Additionally, most damage seems to have occurred to the cloverleaf itself, rather than the straight sections of the two highways. Finally, it is likely that the road owner made additional repair costs beyond what was funded using the 3.8 million euro grant.

4   Discussion

In this work, the object-based approach resulted in lower damage estimates than the grid-based approach. This contrasts with findings of previous studies. For example Jongman et al. (2012) found that "even with the complementary infrastructure data added to CORINE (by adding the road network to the grid), all damage models that include this class *strongly underestimate* the corresponding losses" (2012, p. 3744, brackets and emphasis by us) and that this "is in line with results from earlier studies" (p. 3748). Instead, our findings suggest that grid-based studies using CORINE may *overestimate* infrastructural damage by allocating infrastructural damage to water bodies. However, since the infrastructure contribution to the total damage in these approaches is limited, the estimate of total damage (beyond infrastructure) could still be reliable despite the misallocation in some land cover categories. The grid-based approach using LUISA provided an estimate close to the object-based assessment, indicating that with LUISA, a fair proxy of the total damage to road infrastructure can be obtained.

Within the object-based approach, replacing the Huizinga damage curve with a new set of damage curves resulted in a comparable estimate of the total road damage but distributed a larger share of the damage to motorways and trunk roads. This indicates that the Huizinga infrastructure function is a fair proxy for the average damage to road assets but is unsuitable for assessing damage at the individual road level. The Deggendorf reference case showed that the low-flow curve best resembled the reported flood damage. The new curves also compare reasonably well to damage reported for a Missouri River flood in in Iowa, United States of America (Vennapusa et al., 2013). In order to compare our curves to the damage reported in this study, let us assume a motorway construction costs of 5 million €/km, given that the road design in Iowa is fairly 'simple' (Table 1). Vennapusa et al. report the following motorway damage (Table S18): for clean-up costs: 18,000-65,000 €/km, which is in the order 1% (of 5 million €); for minor up till major repair works: 54,000-388,000 €/km, which is in the order of 1-10%; and for complete reconstruction of a motorway: 5.8 million €/km, which is in the order of 100% of construction costs. A general limitation of our approach is that the flood hazard data used is relatively coarse compared to the high-resolution road segments. In some locations this overestimates the damage, e.g. in a sharp bend a road is falsely overlapped by a river raster cell; in other locations this underestimates the damage, e.g. when a local road depression in reality floods deeper than suggested by the relatively coarse elevation model used to construct the hazard data.

European flood risk studies estimate the total river flood risk aggregated over all land cover types at 4-6 billion €/y (Alfieri et al., 2016b; Jongman et al., 2014), which resembles the reported damage (Paprotny et al., 2018). Our estimate of road damage of 230 million €/y is in the order of 3.8% (of 6 billion) to 5.8% (of 4 billion) of total damage. This infrastructure share of total flood damage is usually in the order of 5-10% (e.g. Pardoe, 2011, as cited by Jongman et al., 2012). Using grid-based

models, Jongman et al. find 8.9%, 2.6% and 8.9% for a flood in Carlisle, for which 11.9% was reported. In specific cases, the damage may be much higher: Jongman et al. (2012) also find values of 18%, 5%, 17% and 3% for a flood in Eilenburg, for which 50% was reported. This made Bubeck et al. (2019) suggest that infrastructural losses may amount up till 60% of total damage. Our results however, suggest that such a high value should be seen as an exception; usually the infrastructure percentage of total damage is much lower. We also perceive the estimate of Bubeck et al. (2019) for the damage to railway infrastructure (11% - 14% of overall flood losses) as being on the high side, given that we find a percentage of only 4-6% for road infrastructure (with the same hazard data) and given that rail damage is usually smaller than road damage (Doll et al., 2014).

Our estimate of 230 million €/y, and 90% confidence interval of 89-373 million €/y is lower than the 660 million €/y reported by Enei et al. (2011). They used an elasticity model linking meteorological indices to road vulnerability data derived from literature. This accounted for the aging of infrastructure, so that the costs attributed to flood damage are lower than the unit replacement costs. However, they included damage caused by landslides as well as damage to bridges, whereas we only look at the impact of floods, and excluded damage to bridges.

Considering that other studies find higher values, could we have underestimated the damage? On the one hand, this seems not to be the case. Firstly, the estimated size of total damage costs for the reference event is at the lower range of our damage estimate. Secondly, it can be argued that places for which our model calculates large damage could be more flood-proofed than what was incorporated in our damage curves. For example, large damage is found for roads along rivers, located in flat flood plains between mountains. In these very vulnerable places, the design standards of the roads may be higher than of the average European road; the road could be extra protected in anticipation of the flood events. Thirdly, road segments that follow a meandering river are sometimes accidently intersected by the relatively coarse flood hazard grid, whereas they do not flood. This makes our model more likely to overestimate than to underestimate the damage.

On the other hand, there are reasons to think that the actual river flood damage is larger than predicted by our model. Firstly, we have limited ourselves to large river floods represented in the flood hazard maps, thereby omitting floods originating from small catchments (<500 km^2). In hilly terrain, flash floods and associated landslides in these smaller catchments can locally cause large damage to road infrastructure, not the least because the flow velocities may exceed what was anticipated in our high-flow curve. Secondly, our study omitted additional damage originating from junctions, viaducts, bridges and tunnels, whereas these could contribute significantly to overall damage. For the reference event, damage to the cloverleaf seems to have contributed most to the overall damage. Similarly, a main source of the exceptionally large damage for the Eilenburg case reported by Jongman et al. (2012) was the collapse of a bridge.

Finally, we would like to emphasize that one should take caution when applying our newly developed damage curves in their own study. We urge to always evaluate the local situation, damage accounting principle and consistency with the hazard data when choosing the most applicable curve. We consider our study to be another step forward in high-resolution risk modelling for transport infrastructure, and ask the community to further calibrate (and validate) the curves, when more empirical data is available. For this, the data in the SI can serve as a reference.

5 Conclusion

This study introduced an object-based approach to modelling the river flood risk of European road infrastructure. This enabled a comparison with the commonly used grid-based approaches, which clearly have difficulties to accurately estimate damage to line infrastructure: road infrastructure may either be overlooked or overestimated by attributing infrastructural damage to the wrong land use types. Also, the study introduced a new set of damage curves which puts the frequently used Huizinga curves in perspective. The expected annual damage from river floods to the road network is 230 million €/y, which is well below the grid-based estimates with CORINE (536 million €/y) and LUISA (301 million €/y). Additionally, we showcased how the object-based approach can be used to identify flood hotspots in the European road network, for which the grid-based approach was unsuitable. This generalized approach can potentially be used for other hazards such as coastal and pluvial floods. We especially recommend the investigation of the damage caused by flash floods and associated landslides in hilly terrain, because the flow velocities and resulting damages seem to exceed what we observed for large scale river flooding.

The model introduced in this study could be a starting point for further analysis. First, the flood hazard data can be easily substituted with (smaller-scale) high-resolution data, to fully exploit the level of detail offered by the OSM exposure dataset. In combination with higher-resolution flood hazard data, it is worth to investigate if splitting the OSM road segments in smaller subsegments can further improve the object-based approach. Second, local scale case studies are required to validate the proposed damage curves. Currently, very little road flood damage case studies are described in the literature, collection of such data by road operators and academia should be a research priority because the absence of damage data hampers the validation of the models. Third, because road flood damage is very sensitive to uncertainty in flood velocity, accounting for this parameter could improve the predictive capacity of the model. Fourth, an object-based approach can be used to investigate potential damage to bridges, culverts, tunnels, viaducts and junctions.

In the broader context of risk assessments for roads, this study offers a practical method for large (continental) scale risk assessment without compromising the resolution of the exposure data, hence suitable for hotspot identification. Both continental scale and local scale assessments can use the same framework, only the hazard data needs to be substituted with high-resolution local data. The results are presented on the level of individual road segments which meets a demand of road owners (Bles et al., 2016) by providing immediate perspective of action. This bridges the gap between detailed local-scale object-based studies (e.g. Hackl et al., 2018) and coarse continental-scale econometric (e.g. Doll et al., 2014) or grid-based studies (e.g. Dottori et al., 2020). Finally, the object-based approach offers an indispensable level of detail for two types of analysis. First, damage from network disruptions and indirect economic effects can be studied using the same road network as used in the analysis of direct damage. Network graphs can be directly constructed from the OSM road objects, which is impossible with a grid-based approach. Second, flood risk studies are increasingly used to support decision making on climate adaptation. The unique characteristics of each road segment are highly relevant for targeted climate resilient infrastructure investments and can only be captured in a road specific, object-based approach.

Supplementary information

This paper contains supplementary information with model settings, road construction and maintenance cost data, the new damage curves, and detailed descriptions of the model results. These results include a high-resolution map and shapefile of the flood risk of motorways and trunk roads in the European road network.

Code and data availability

The Python code for the object-based model can be retrieved from github.com/keesvanginkel/OSdaMage. The SI contains a shapefile with the model outputs for the European highway network (motorways and trunk roads). Data for all OSM road classes per NUTS-3 region can be retrieved from the authors.

The JRC flood hazard maps used in this work are available for download and reuse at the JRC Data Catalogue at this link: https://data.jrc.ec.europa.eu/dataset/1d128b6c-a4ee-4858-9e34-6210707f3c81.

Funding

This paper has received funding from the European Union's Horizon 2020 research and innovation programme under grant agreement No 776479 for the project CO-designing the Assessment of Climate CHange costs. https://www.coacch.eu/. Elco Koks was further supported by the Netherlands Organization for Scientific Research NWO (Grant No VI.Veni.194.033).

Author contribution

KvG prepared the manuscript with contributions from all co-authors. FD, LA and LF prepared the flood hazard maps and damage maps of the grid-based approach. EK developed the object-based approach, KvG tailored it to the European context. KvG and EK carried out the computational experiments and investigated, validated, and visualised the results. All authors approved the final publication.

Competing interests

The authors declare that they have no conflict of interest.

Acknowledgements

We thank the *Dutch Ministry of Infrastructure and Water Management, Rijkswaterstaat* for providing insight into the cost structure of motorways, and the *Bavarian State Ministry for Housing, Construction and Transport* for providing the data on flood damage in Deggendorf. Deltares colleagues Thomas Bles, Ana Laura Costa and Dennis Wagenaar contributed to shaping the new damage curves. Aoife O'Connor assisted in collecting data on road construction costs.

References

Albano, R., Mancusi, L., Sole, A. and Adamowski, J.: FloodRisk: a collaborative, free and open-source

software for flood risk analysis, Geomatics, Nat. Hazards Risk, 8(2), 1812–1832,
doi:10.1080/19475705.2017.1388854, 2017.

Alfieri, L., Salamon, P., Bianchi, A., Neal, J., Bates, P. and Feyen, L.: Advances in pan-European flood
hazard mapping, Hydrol. Process., 28(13), 4067–4077, doi:10.1002/hyp.9947, 2014.

Alfieri, L., Feyen, L., Dottori, F. and Bianchi, A.: Ensemble flood risk assessment in Europe under high
end climate scenarios, Glob. Environ. Chang., 35, 199–212, doi:10.1016/j.gloenvcha.2015.09.004,
2015.

Alfieri, L., Feyen, L. and Di Baldassarre, G.: Increasing flood risk under climate change: a pan-
European assessment of the benefits of four adaptation strategies, Clim. Change, 136(3–4), 507–521,
doi:10.1007/s10584-016-1641-1, 2016a.

Alfieri, L., Feyen, L., Salamon, P., Thielen, J., Bianchi, A., Dottori, F. and Burek, P.: Modelling the
socio-economic impact of river floods in Europe, Nat. Hazards Earth Syst. Sci., 16(6), 1401–1411,
doi:10.5194/nhess-16-1401-2016, 2016b.

Alfieri, L., Dottori, F., Betts, R., Salamon, P. and Feyen, L.: Multi-Model Projections of River Flood Risk
in Europe under Global Warming, Climate, 6(1), 6, doi:10.3390/cli6010006, 2018.

Amadio, M., Mysiak, J., Carrera, L. and Koks, E.: Improving flood damage assessment models in Italy,
Nat. Hazards, 82(3), 2075–2088, doi:10.1007/s11069-016-2286-0, 2016.

Amadio, M., Rita Scorzini, A., Carisi, F., Essenfelder, H. A., Domeneghetti, A., Mysiak, J. and
Castellarin, A.: Testing empirical and synthetic flood damage models: The case of Italy, Nat. Hazards
Earth Syst. Sci., 19(3), 661–678, doi:10.5194/nhess-19-661-2019, 2019.

Archondo-Callao, R., Roads works costs per km from World Bank Reports (presentation). April, 2000.

Arnell, N. W. and Gosling, S. N.: The impacts of climate change on river flood risk at the global scale,
Clim. Change, 134(3), 387–401, doi:10.1007/s10584-014-1084-5, 2016.

Barrington-Leigh, C. and Millard-Ball, A.: The world's user-generated road map is more than 80%
complete, PLoS One, 12(8), 1–20, doi:10.1371/journal.pone.0180698, 2017.

Bates, P. D., Horritt, M. S., & Fewtrell, T. J.: A simple inertial formulation of the shallow water
equations for efficient two-dimensional flood inundation modelling. J. Hydrol. 387(1-2), 33-45, doi:
10.1016/j.jhydrol.2010.03.027

Blanc-Brude, F., Goldsmith, H. and Välilä, T.: Ex Ante Construction Costs in the European Road Sector:
A Comparison of Public-Private Partnerships and Traditional Public Procurement (Economic and
Financial Report 2006/01), Europ. Invest. Bank, Kirchberg., 2006.

Bles, T., Bessembinder, J., Chevreuil, M., Danielsson, P., Falemo, S., Venmans, A., Ennesser, Y.,
Löfroth, H.: Climate change risk assessment and adaptation for roads – results of the ROADAPT
project, in: Transportation Research Procedia 14, doi:10.1016/j.trpro.2016.05.041, 6th Transport
Research Arena, Warsaw, Poland, 18-21 April 2016, 58-67, 2016.

Bouwer, L., Capriolo, A., Chiabai,. A., Foudi, S., Garrote, L., Harmackova, Z.V., Iglesias, A., Jeuken, A.,
Olazabal, M., Spadaro, J., Taylor, T., Zandersen, M.: Upscaling the impacts of climate change in
different sectors and adaptation strategies, in: Adapting to climate change in Europe, edited by:
Sanderson, H., Hilden, M., Russel, D., Penha-Lopes, G., Capriolo, A., Elsevier, Amsterdam, The
Netherlands, 173-243, doi: 10.1016/B978-0-12-849887-3.00001-0, 2018.

720 Bubeck, P., Dillenardt, L., Alfieri, L., Feyen, L., Thieken, A. H. and Kellermann, P.: Global warming to increase flood risk on European railways, Clim. Change, 155(1), 19–36, doi:10.1007/s10584-019-02434-5, 2019.

Büttner, G., Soukup, T. and Kosztra, B.: CLC2012. Addendum to CLC2006 Technical Guidelines, European Environment Agency, Copenhagen, Denmark, 35 pp., 2014.

Carisi, F., Schröter, K., Domeneghetti, A., Kreibich, H. and Castellarin, A.: Development and 725 assessment of uni- and multivariable flood loss models for Emilia-Romagna (Italy), Nat. Hazards Earth Syst. Sci., 18(7), 2057–2079, doi:10.5194/nhess-18-2057-2018, 2018.

Carruthers, R.: What prospects for transport infrastructure and impacts on growth in southern and eastern Mediterranean countries?, MEDPRO report No. 3, 2013.

Chang, H., Lafrenz, M., Jung, I.-W., Figliozzi, M., Platman, D., Pederson, C.: Potential Impacts of 730 Climate Change on Flood-Induced Travel Disruptions: A Case Study of Portland, Oregon, USA, Ann. Assoc. Am. Geogr., 100, 938–952, doi: 10.1080/00045608.2010.497110, 2010.

Dankers, R. and Feyen, L.: Climate change impact on flood hazard in Europe: An assessment based on high-resolution climate simulations, J. Geophys. Res. Atmos., 113(19), 1–17, doi:10.1029/2007JD009719, 2008.

735 Doll, C., Klug, S. and Enei, R.: Large and small numbers: options for quantifying the costs of extremes on transport now and in 40 years, Nat. Hazards, 72(1), 211–239, doi:10.1007/s11069-013-0821-9, 2014.

Dottori, F., Alfieri, L., Bianchi, A., Skoien, J., and Salamon, P.: A new dataset of river flood hazard maps for Europe and the Mediterranean Basin region, Earth Syst. Sci. Data Discuss, [preprint], 740 doi.:10.5194/essd-2020-313, in review, 2021.

Dottori, F., Martina, M. L. V. and Figueiredo, R.: A methodology for flood susceptibility and vulnerability analysis in complex flood scenarios, J. Flood Risk Manag., 11, S632–S645, doi:10.1111/jfr3.12234, 2018a.

Dottori, F., Szewczyk, W., Ciscar, J. C., Zhao, F., Alfieri, L., Hirabayashi, Y., Bianchi, A., Mongelli, I., 745 Frieler, K., Betts, R. A. and Feyen, L.: Increased human and economic losses from river flooding with anthropogenic warming, Nat. Clim. Chang., 8(9), 781–786, doi:10.1038/s41558-018-0257-z, 2018b.

Dottori, F., Mentaschi, L., Bianchi, A., Alfieri, L., and Feyen L.: Adapting to rising river flood risk in the EU under climate change, Publications Office of the European Union, Luxembourg, doi: 10.2760/14505, 2020.

750 Enei, R., Doll, C., Klug, S., Partzsch, I., Sedlacek, N., Kiel, J., Nesterova, N., Rudzikaite, L., Papanikolaou, A. and Mitsakis, V.: Weather Extremes: Assessment of Impacts on Transport Systems and Hazards for European Regions. Deliverable 2: Vulnerability of Transport systems., Karlsruhe, Germany, 2011.

ECA: Are EU Cohesion Policy funds well spent on roads? Special Report No 5/2013, European Court of Auditors, Luxembourg, Luxembourg, https://doi.org/10.2865/71435, 2013.

755 EEA: The thematic accuracy of Corine land cover 2000 – assessment using LUCAS, Technical report No 7/2006, European Environment Agency, Copenhagen, Denmark, 2006.

Eurostat: Real GDP per capita, Statistical Office of the European Union, sdg_08_10, 2019.

Federal Ministry of Transport and Digital Infrastructure: Verkehrsinvestitionsbericht für das berichtsjahr 2016, Berlin, Germany, 2016.

760   Gil, J. and Steinbach, P.: From flood risk to indirect flood impact: Evaluation of street network performance for effective management, response and repair, WIT Trans. Ecol. Environ., 118, 335–344, doi:10.2495/FRIAR080321, 2008.

Hackl, J., Heitzler, M., Lam, J. C., Adey, B. and Hurni, L.: Deliverable 4.2 of the INFRARISK project (Novel indicators for identifying critical infrastructure at risk from natural hazards), Zürich,
765   Switzerland, 2016.

Hackl, J., Lam, J. C., Heitzler, M., Adey, B. T., & Hurni, L.: Estimating network related risks: A methodology and an application in the transport sector, Nat. Hazards Earth Syst. Sci., 18(8), 2273–2293, doi: 10.5194/nhess-18-2273-2018, 2018.

Heralova, R. S., Hromada, E. and Johnston, H.: Cost structure of the highway projects in the Czech
770   Republic, Procedia Eng., 85, 222–230, doi:10.1016/j.proeng.2014.10.547, 2014.

Heralova, R. S., Hromada, E. and Johnston, H.: Cost structure of the highway projects in the Czech Republic, Procedia Eng., 85, 222–230, doi:10.1016/j.proeng.2014.10.547, 2014.

Hirabayashi, Y., Mahendran, R., Koirala, S., Konoshima, L., Yamazaki, D., Watanabe, S., Kim, H. and Kanae, S.: Global flood risk under climate change, Nat. Clim. Chang., 3(9), 816–821,
775   doi:10.1038/nclimate1911, 2013.

Huizinga, H. J.: Flood damage functions for EU member states, HKV Consultants, Lelystad, The Netherlands, 2007.

Huizinga, J., de Moel, H. and Szewczyk, W.: Global flood depth-damage functions. Methodology and database with guidelines, Publications Office of the European Union, Luxembourg, doi:
780   10.2760/16510, 2017.

International Sava River Basin Commission: Preliminary Flood Risk Assessment in the Sava River Basin, Zagreb, Croatia, 2014.

Jongman, B., Kreibich, H., Apel, H., Barredo, J. I., Bates, P. D., Feyen, L., Gericke, A., Neal, J., Aerts, J. C. J. H. and Ward, P. J.: Comparative flood damage model assessment: Towards a European approach,
785   Nat. Hazards Earth Syst. Sci., 12(12), 3733–3752, doi:10.5194/nhess-12-3733-2012, 2012.

Jongman, B., Hochrainer-Stigler, S., Feyen, L., Aerts, J. C. J. H., Mechler, R., Botzen, W. J. W., Bouwer, L. M., Pflug, G., Rojas, R. and Ward, P. J.: Increasing stress on disaster-risk finance due to large floods, Nat. Clim. Chang., 4(4), 264–268, doi:10.1038/nclimate2124, 2014.

Jonkman, S. N., and Kelman, I.: An Analysis of the Causes and Circumstances of Flood Disaster Deaths.
790   Disasters 29(1), 75-79, doi: 10.1111/j.0361-3666.2005.00275.x, 2005

Jonkman, S.N., Bočkarjova, M., Kok, M., Bernardini, P., Integrated hydrodynamic and economic modelling of flood damage in the Netherlands, Ecol. Econ., 66, 77–90, doi:10.1016/j.ecolecon.2007.12.022, 2008.

van der Knijff, J. M., Younis, J. and De Roo, A. P. J.: LISFLOOD: a GIS-based distributed model for river
795   basin scale water balance and flood simulation, Int. J. Geogr. Inf. Sci., 24(2), 189–212, doi:10.1080/13658810802549154, 2010.

Koks, E. E., Rozenberg, J., Zorn, C., Tariverdi, M., Vousdoukas, M., Fraser, S. A., Hall, J. W. and

Hallegatte, S.: A global multi-hazard risk analysis of road and railway infrastructure assets, Nat. Commun., 10(1), 1–11, doi:10.1038/s41467-019-10442-3, 2019.

800 Kreibich, H., Piroth, K., Seifert, I., Maiwald, H., Kunert, U., Schwarz, J., Merz, B. and Thieken, A. H.: Is flow velocity a significant parameter in flood damage modelling?, Nat. Hazards Earth Syst. Sci., 9(5), 1679–1692, doi:10.5194/nhess-9-1679-2009, 2009.

Kron, W.: Flood Risk = Hazard x Values x Vulnerability, Water Int., 30(1), 58–68, doi:10.1080/02508060508691837, 2005.

805 Kundzewicz, Z. W., Krysanova, V., Dankers, R., Hirabayashi, Y., Kanae, S., Hattermann, F. F., Huang, S., Milly, P. C. D., Stoffel, M., Driessen, P. P. J., Matczak, P., Quevauviller, P. and Schellnhuber, H. J.: Differences in flood hazard projections in Europe–their causes and consequences for decision making, Hydrol. Sci. J., 62(1), 1–14, doi:10.1080/02626667.2016.1241398, 2017.

Lamb, R., Garside, P., Pant, R. and Hall, J. W.: A Probabilistic Model of the Economic Risk to Britain's
810 Railway Network from Bridge Scour During Floods, Risk Anal., 39(11), doi:10.1111/risa.13370, 2019.

Lincke, D., Hinkel, H., van Ginkel, K., Jeuken, A., Botzen, W., Tesselaar, M., Scoccimarro, E., Ignjacevic, P.: Impacts on infrastructure, built environment and transport, Deliverable 2.3 of the COACCH project, 78 pp., 2019.

Lugeri, N., Kundzewicz, Z. W., Genovese, E., Hochrainer, S. and Radziejewski, M.: River flood risk and
815 adaptation in Europe-assessment of the present status, Mitig. Adapt. Strateg. Glob. Chang., 15(7), 621–639, doi:10.1007/s11027-009-9211-8, 2010.

Meneses, B. M., Pereira, S. and Reis, E.: Effects of different land use and land cover data on the landslide susceptibility zonation of road networks, Nat. Hazards Earth Syst. Sci., 19(3), 471–487, doi:10.5194/nhess-19-471-2019, 2019.

820 Merz, B., Kreibich, H., Schwarze, R. and Thieken, A.: Assessment of economic flood damage, Nat. Hazards Earth Syst. Sci., 10(8), 1697–1724, doi:10.5194/nhess-10-1697-2010, 2010.

de Moel, H., van Alphen, J., & Aerts, J. C. J. H.: Flood maps in Europe - methods, availability and use, Nat. Hazards Earth Syst. Sci., 9(2), 289–301, doi:10.5194/nhess-9-289-2009, 2009.

de Moel, H. and Aerts, J. C. J. H.: Effect of uncertainty in land use, damage models and inundation
825 depth on flood damage estimates, Nat. Hazards, 58(1), 407–425, doi:10.1007/s11069-010-9675-6, 2011.

de Moel, H., Jongman, B., Kreibich, H., Merz, B., Penning-Rowsell, E. and Ward, P. J.: Flood risk assessments at different spatial scales, Mitig. Adapt. Strateg. Glob. Chang., 20(6), 865–890, doi:10.1007/s11027-015-9654-z, 2015.

830 Nijland, H., Wortelboer-van Donselaar, P. M., Korteweg, J. A. C. and Snellen, D.: 'Met de kennis van nu': leren van evalueren Een casestudy: A5 Verlengde Westrandweg, Netherlands Environmental Assessment Agency, The Hague, The Netherlands, 2010.

Olsen, A. S., Zhou, Q., Linde, J. J., & Arnbjerg-Nielsen, K.: Comparing methods of calculating expected annual damage in urban pluvial flood risk assessments, Water, 7(1), 255–270,
835 doi.org/10.3390/w7010255, 2015.

OpenStreetMap contributors: http://openstreetmap.org, Europe dump of 7 januari 2019.

Paprotny, D., Sebastian, A., Morales-Nápoles, O. and Jonkman, S. N.: Trends in flood losses in Europe

over the past 150 years, Nat. Commun., 9(1), doi:10.1038/s41467-018-04253-1, 2018.

Peduzzi, P., Dao, H., Herold, C. and Mouton, F.: Assessing global exposure and vulnerability towards natural hazards: the Disaster Risk Index, Nat. Hazards Earth Syst. Sci., 9(4), 1149–1159, doi:10.5194/nhess-9-1149-2009, 2009.

Prahl, B. F., Boettle, M., Costa, L., Kropp, J. P. and Rybski, D.: Damage and protection cost curves for coastal floods within the 600 largest European cities, Sci. Data, 5(1), 180034, doi:10.1038/sdata.2018.34, 2018.

Pregnolato, M.: Bridge safety is not for granted – A novel approach to bridge management, Eng. Struct., 196, 109193, doi:10.1016/j.engstruct.2019.05.035, 2019.

Pryzluski, V., Hallegatte, S., Tomozeiu, R., Cacciamani, C., Pavan, V. and Doll, C.: Weather Trends and Economy-Wide Impacts (Deliverable 1 within the research project WEATHER (Weather Extremes: Impacts on Transport Systems and Hazards for European Regions), Karlsruhe, Germany, 2012.

Reese, S., Markau, H., Sterr, H.: Mikroskalige Evaluation der Risiken in überflutungsgefährdeten Küstenniederungen, Forschungs- und Technologiezentrum Westküste, E34893, Kiel, Germany, 2003.

Rogowsky, W.: Erfahrungsbericht vor Ort beim Hochwasser 2013 in Bayern, Internationales Wasserbau-Symposium Aachen (IWASA), pp. 1–10, Aachen, Germany, 2016.

Rosina, K., Batista e Silva, F., Vizcaino, P., Marín Herrera, M., Freire, S. and Schiavina, M.: Increasing the detail of European land use/cover data by combining heterogeneous data sets, Int. J. Digit. Earth, 8947, doi:10.1080/17538947.2018.1550119, 2018.

Scussolini, P., Aerts, J. C. J. H., Jongman, B., Bouwer, L. M., Winsemius, H. C., De Moel, H., and Ward, P. J.: FLOPROS: an evolving global database of flood protection standards, Nat. Hazards Earth Syst. Sci., 16(5), 1049–1061. doi:10.5194/nhess-16-1049-2016, 2016.

Serinaldi, F. and Kilsby, C. G.: A Blueprint for Full Collective Flood Risk Estimation: Demonstration for European River Flooding, Risk Anal., 37(10), 1958–1976, doi:10.1111/risa.12747, 2017.

Sohn, J.: Evaluating the significance of highway network links under the flood damage: An accessibility approach, Transport Res A-Pol, 40(6), 491-506, doi: 10.1016/j.tra.2005.08.006, 2006.

Strappazzon, Q. and Pierlot, D.: Stratégie locale de Gestion du Risque Inondation: Grenoble – Voiron., Grenoble, France, 2017.

Suarez, P., Anderson, W., Mahal, V., Lakshmanan, T.R., Impacts of flooding and climate change on urban transportation: A systemwide performance assessment of the Boston Metro Area, Transp. Res. Part D Transp. Environ., 10, 231–244, doi:10.1016/j.trd.2005.04.007, 2005.

Thieken, a. H., Ackermann, V., Elmer, F., Kreibich, H., Kuhlmann, B., Kunert, U., Maiwald, H., Merz, B., Müller, M., Piroth, K., Schwarz, J., Schwarze, R., Seifert, I. and Seifert, J.: Methods for the evaluation of direct and indirect flood losses, in RIMAX Contributions at the 4th International Symposium on Flood Defence (ISFD4), pp. 1–10, 2009.

Thielen, J., Bartholmes, J., Ramos, M.-H. and de Roo, A.: The European Flood Alert System – Part 1: Concept and development, Hydrol. Earth Syst. Sci., 13(2), 125–140, doi:10.5194/hess-13-125-2009, 2009.

Vennapusa, P. K. R., White, D. J. and Miller, D. K.: Western Iowa Missouri River Flooding — Geo-Infrastructure Damage Assessment, Repair and Mitigation Strategies, Iowa State Univ., InTrans

Project Reports 97, 2013.

Ward, P. J., Jongman, B., Weiland, F. S., Bouwman, A., van Beek, R., Bierkens, M. F. P., Ligtvoet, W. and Winsemius, H. C.: Assessing flood risk at the global scale: Model setup, results, and sensitivity, Environ. Res. Lett., 8(4), 44019, doi:10.1088/1748-9326/8/4/044019, 2013.

Winsemius, H. C., Van Beek, L. P. H., Jongman, B., Ward, P. J. and Bouwman, A.: A framework for global river flood risk assessments, Hydrol. Earth Syst. Sci., 17(5), 1871–1892, doi:10.5194/hess-17-1871-2013, 2013.

880

885